Journal of Alloys and Compounds 509 (2011) 3306–3309

Contents lists available at ScienceDirect

Journal of Alloys and Compounds

journal homepage: www.elsevier.com/locate/jallcom

Sublimation sandwich route to ultralong zinc-blende ZnSe nanowires and the cathodoluminescence properties of individual nanowires

H.W. Zhu[a], P.G. Li[a], M. Lei[a], L.H. Li[b], S.L. Wang[a], W.H. Tang[a,*]

[a] Department of Physics, Center for Optoelectronics Materials and Devices, Zhejiang Sci-Tech University, Xiasha College Park, Hangzhou 310018, China
[b] Department of Geology, Geography, and Physics, University of Tennessee at Martin, 215 Johnson EPS Bldg, Martin, TN 38238, USA

ARTICLE INFO

Article history:
Received 15 October 2010
Received in revised form 6 December 2010
Accepted 7 December 2010
Available online 14 December 2010

Keywords:
Semiconductors
Nanostructured materials
Optical property

ABSTRACT

Sublimation sandwich method (SSM) was developed to fabricate ZnSe nanowires assisted by Au-catalytic vapor–liquid–solid (VLS) process. The ZnSe nanowires have zinc-blende structure and the length is ultralong, up to tens of micrometers. High-resolution transmission electron microscopic (HRTEM) investigations reveal that there are two types of nanowires: well crystalline nanowires and poor crystalline nanowires with high density of bulk defects e.g. stacking faults, dislocations and twinning defects. The cathodoluminescence spectra indicate significant difference in optical properties of these two types of nanowires. We deduce that V_{Zn} and Zn_i are the main reason for the deep defects related green–red emission observed in well crystalline nanowires, while the bulk defects in the poor crystalline nanowires should be responsible for the deep defects related emissions centered at 515 and 604 nm.

1. Introduction

One-dimensional (1D) II–VI semiconductor nanowires have attracted much attention due to their unique electrical and optical properties and potential applications in various optoelectronic and electronic nanodevices [1–5]. Among these II–VI semiconductors, ZnSe nanowires are promising materials as photodetectors, light-emitting diodes and laser diodes due to its wide bandgap of *ca.* 2.7 eV (460 nm) and large exciton binding energy of 21 meV [6–10]. The syntheses and properties of ZnSe nanowires have been extensively studied to now [8,11–14]. Recently, some conventional technologies of film, including metal-organic chemical vapor deposition (MOCVD) [15–17], laser ablation (LA) [18], molecular beam epitaxy (MBE) [19,20], and atomic layer deposition (ALD) [21] had been developed to synthesize the ZnSe nanowires, demonstrating the possibility of the integration of the ZnSe thin films and 1D nanowires technology by the same routes. Nevertheless, these technologies are high expensive and the length of the as-synthesized nanowires is too short to be applied in nanofabrications. Sublimation sandwich method (SSM) is a modified sublimation technique which was introduced to grow single-crystal SiC and GaN thick films [22–24]. The main feature of SSM is the closer distance of about several millimeters between source and substrate, which can intensify mass transport during the growth of film [25]. For example, The SSM for growth of monocrystalline SiC was shown to be promising technique to obtain material with significantly lower density of dislocations and micropipes [26]. In particular, sufficiently thick (e.g. 1–2 mm) epitaxial layers of SiC free from micropores and micropipes were obtained using the SSM. Recently, the SSM had been successfully applied in synthesis of III–V group nanowires e.g. GaN assisted by Au catalysts [27,28]. We deduced that the SST may be extended to fabricate some II–VI semiconductor nanowires. Here, we reported a facile SSM to fabricate ultralong zinc-blende ZnSe nanowires on the Au-coated Si substrates. The microstructure and single nanowire related CL properties of the ZnSe nanowires were investigated in detail and presented some novel features on the ZnSe naowires.

2. Experimental

The container used here is a columnar graphite box with inner depth of about 30 mm. A hole with diameter 6 mm excavated in the lid of the box was used to place Si substrates. On the wall of the box, two gaps with width of 12 mm and high of 6 mm were excavated in order to introduce the desired protected atmosphere into the growth cell. Au-coated Si (1 0 0) substrates without any pretreatment are used for the growth of ZnSe nanowires. In the experiment, the Au-coated Si substrates were supported by the lid. Commercial ZnSe powder is placed in the container as source with a distance of about 25 mm upright away from substrates. Then, the growth cell loading source and substrates were placed into an upright quartz chemical vapor deposition system, forming an upright SSM configuration. After flushed with Ar flow to remove the remaining air in the furnace, the whole system was heated to 800 °C and kept the peak temperature for half an hour under mixed Ar/H_2 atmosphere with ratio 9:1 at flow rate of 150 sccm. Finally the furnace was cooled to room temperature and the deposits were taken out for further characterization.

The crystal structure of the product was analyzed using a rotating anode Rigaku (Tokyo, Japan) D/max-2400 X-ray diffractometer with Cu Kα radiation. The morphology of the product was characterized by Hitach (Tokyo, Japan) S-4200 field emission scanning electron microscope (FE-SEM) equipped with energy-dispersive

* Corresponding author. Tel.: +86 571 86843222; fax: +86 571 86843222.
E-mail address: whtang@zstu.edu.cn (W.H. Tang).

0925-8388/$ – see front matter © 2010 Elsevier B.V. All rights reserved.
doi:10.1016/j.jallcom.2010.12.037

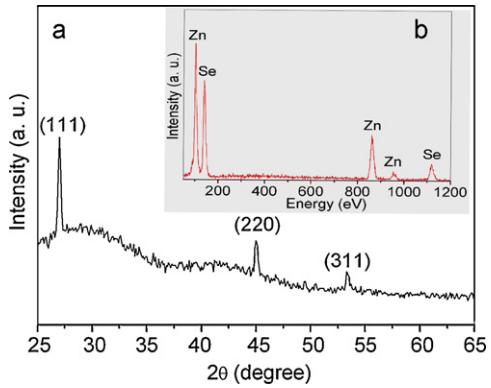

Fig. 1. (a) XRD patterns of the ZnSe nanowires; (b) EDS spectrum of the ZnSe nanowires.

X-ray spectroscopy (EDS). The microstructure of the product was examined by transmission electron microscopy (TEM, Philips CM 12 at 100 kV) and high-resolution TEM (HRTEM, Philips CM 12 at 200 kV). The cathodoluminescence (CL) studies of individual nanowire were performed in the scanning electron microscope equipped with an Oxford Instruments MonoCL2 spectrometer at room temperature. The focused electron beam was scanned over the surface, and the emitted light was collected with a parabolic aluminum mirror and guided to the slit of a grating monochromator. The working probe current is 200 pA for the CL measurement.

3. Results and discussion

The phase structure of the as-deposited product on Au-coated Si substrates is first characterized by XRD, as shown in Fig. 1a. All diffraction peaks can be indexed as (1 1 1), (2 2 0) and (3 1 1) on the basis of zinc-blende ZnSe, and no other peaks from impurities are detected. The lattice parameters of the deposit are calculated to be $a = 5.676$ Å, well consistent with that of the standard cubic ZnSe (ICDD-PDF No. 37-1463). The corresponding EDS spectrum (Fig. 1b) reveals that the deposit mainly consists of Zn and Se elements, which further demonstrates that the deposit is zinc-blende ZnSe with high purity. The overall SEM image (Fig. 2a) clearly shows that the deposit consists of a large amount of straight nanowires with length up to several tens of micrometers. The enlarged SEM image of the deposit (Fig. 2b) indicates that the average diameter of the nanowires is *ca.* 150 nm and each of them has a smooth surface.

The microstructure of the deposits was further investigated by utilizing TEM and high-resolution TEM (HRTEM). Fig. 3a shows TEM image of an individual nanowire. The nanowire exhibits smooth surface and a nanoparticle is found to attach on the tip of the nanowire. The nanoparticle is identified as Au–Zn–Se alloy, revealing that the growth process is likely initiated by the well known vapor–liquid–solid (VLS) mechanism. The corresponding EDS spectrum indicates that the nanowire is mainly composed of Zn and Se elements, as shown in Fig. 3b. The atomic ratio of Zn and Se is about 0.993:1, close to the stoichiometric formation of ZnSe. The HRTEM analysis (Fig. 3c) and fast Fourier transform (FFT) (inset of Fig. 3c) reveal that the nanowire is well crystalline and the growth direction is determined to grow along [1 1 1]. No obvious bulk defects such as stacking faults, dislocations and twining defects are observed. Fig. 3d shows morphology of another individual nanowire, respectively, similar to that of the nanowire shown in Fig. 3a. Nevertheless, the corresponding HRTEM image (Fig. 3e) reveals high density of stacking faults and dislocations, as can be further confirmed by the streaks shown in the FFT patterns (inset of Fig. 3e). The twinning defects are also observed. As indexed in Fig. 3f, the growth direction is [1 1 1], and the planar twins are on the {0 2 1} planes.

Fig. 4a shows the CL spectrum of the ZnSe nanowire with well crystalline nature. It is comprised of two emission bands: a weak green emission peak centered at 462 nm (2.68 eV) and a broad, strong green–red emission at 632 nm (1.96 eV). The weak green emission is the characteristic of near band edge (NBE) emission of ZnSe. The broad green–red emission band extending from around 500 to 750 nm is a typical deep defect (DD) related emission. From the HRTEM image of the nanowires (Fig. 3c), no bulk defects such as dislocations, stacking faults and twinning defects are observed. So, we deduce that the origin of green–red emission is attributed to the intrinsic point defects. The intrinsic point defects can be simply divided into four species: Se vacancy (V_{Se}), Zn vacancy (V_{Zn}), Zn interstitial (Zn_i), and Se interstitial (Se_i). The experiment results and theoretic calculations had concluded that V_{Se} is difficult to exist in the ZnSe nanowires due to its high formation energy, and V_{Zn} and/or Zn_i are the most probable point defects in the ZnSe nanowires [29–31]. As confirmed by the EDS analysis (Fig. 3b), Se atoms are a trace of excess in the ZnSe nanowires. So, V_{Zn} and Zn_i are probably responsible for the DD related emission of the stoichiometric nanowires. V_{Zn} act as the acceptor species while Zn_i as the donor species. In the case, all carriers excited to the conduction band almost instantaneously decay to shallow donor levels and recombine with acceptor states emitting photons corresponding to donor–acceptor pair recombination mechanism, which finally results in the broad, strong green–red emission band of the ZnSe nanowires [30–33]. Fig. 4b shows the CL spectrum of another individual nanowire with poor crystallization. It is found that a weak NBE emission band centered at 475 nm (2.61 eV) and two strong DD related emission bands centered at 515 and 604 nm, respectively, are detected in the poor crystalline nanowire. As confirmed by the

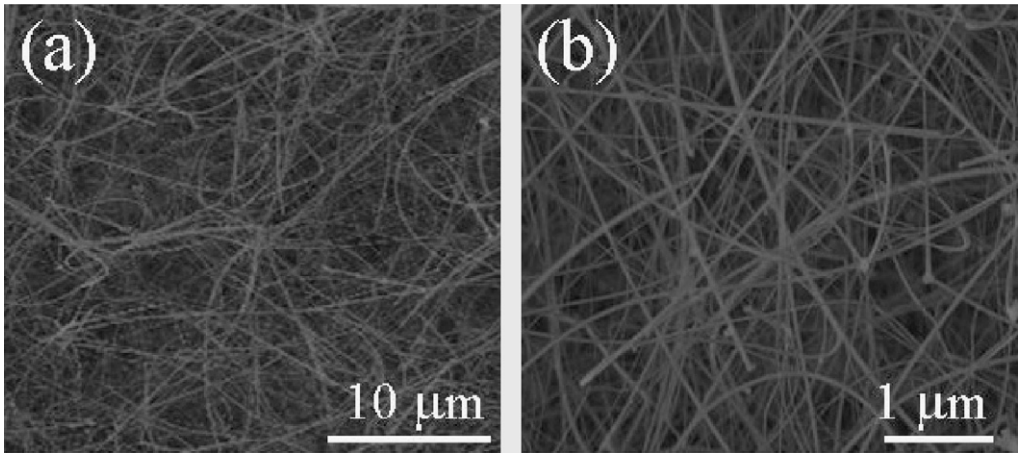

Fig. 2. (a) SEM and (b) enlarged SEM images of the ZnSe nanowires.

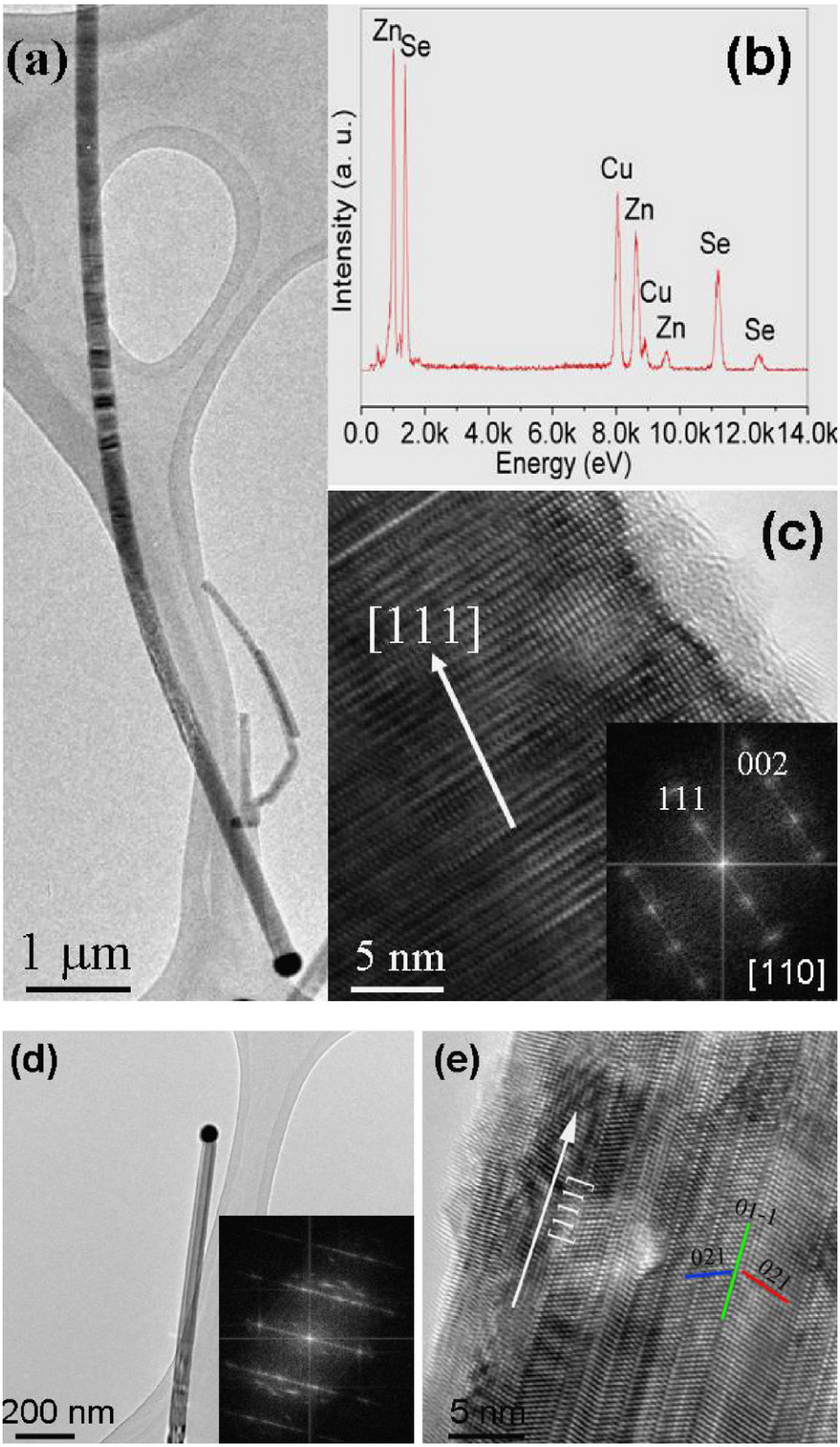

Fig. 3. (a) TEM image of an individual ZnSe nanowire. (b) The corresponding EDS spectrum of the ZnSe nanowire. (c) HRTEM image of the ZnSe nanowire. The inset is the corresponding FFT pattern. (d) TEM image of another individual ZnSe nanowire. The inset is the corresponding FFT pattern. (e) HRTEM image of the ZnSe nanowire.

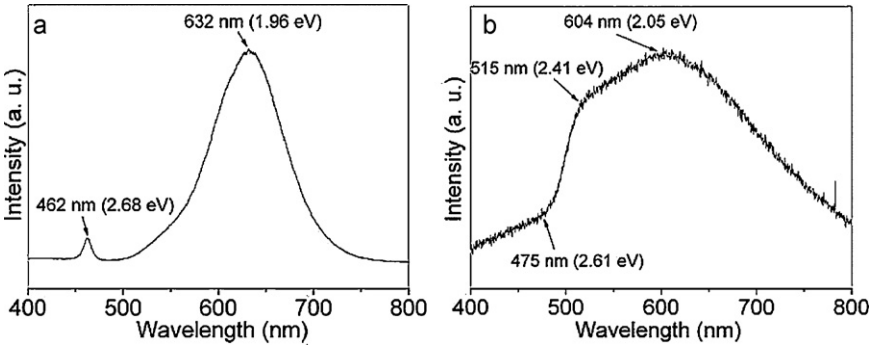

Fig. 4. CL spectra of an individual nanowire with (a) well crystalline nature and (b) high density of bulk defects.

HRTEM investigation (Fig. 3e), high density of dislocation, stacking faults and twinning defects are observed in the nanowires, which should be responsible for the two observed DD emission bands [30,31]. These bulk defects act as deep defect donors and recombine with acceptor states emitting phonons to form new energy level, which results in the two unusual DD emission bands.

4. Conclusions

ZnSe nanowires with high purity have been synthesized using Au as catalysts via a facile sublimation sandwich method. The structural characterization reveals that ZnSe nanowires have zinc-blende structure and the length is ultralong, up to tens of micrometers. HRTEM investigations reveal that there are two types of nanowires: well crystalline nanowires and crystalline nanowires with high density of bulk defects such as stacking faults, dislocations and twinning defects. The corresponding CL spectra indicate a significant difference in optical properties of these two types of nanowires. A weak NBE emission centered at 462 nm and a broad, strong green–red emission at 632 nm are observed in the well crystalline nanowires. We deduce that V_{Zn} and Zn_i are the main reason for the DD related green–red emission. Nevertheless, three emission bands centered at 475, 515 and 604 nm, respectively, are detected in the poor crystalline nanowires with highly dense bulks defects. These bulk defects, e.g. stacking faults, dislocations and twinning defects, should be responsible for the unusual DD emission bands at 515 and 604 nm.

Acknowledgements

This work was financially supported by the 973 Program (Grant No. 2010CB933501), the Innovative Youth Team of Natural Science Foundation of Zhejiang Province (Grant No. R4090058), and the National Natural Science Foundation of China (Grant No. 51072182).

References

[1] X.D. Wang, J.H. Song, J. Liu, Z.L. Wang, Science 316 (2007) 102–105.
[2] L.F. Xi, Y.M. Lam, Chem. Mater. 21 (2009) 3710–3718.
[3] P.X. Cao, Y. Ding, Z.L. Wang, Nano Lett. 9 (2009) 137–143.
[4] Y.C. Li, H.Z. Zhong, R. Li, Y. Zhou, C.H. Yang, Y.F. Li, Adv. Funct. Mater. 16 (2006) 1705–1716.
[5] M.H. Huang, S. Mao, H. Feick, H.Q. Yan, Y.Y. Wu, H. Kind, E. Weber, R. Russo, P.D. Yang, Science 292 (2001) 1897–1899.
[6] R. Rujkorakarn, A.J. Nelson, J. Appl. Phys. 87 (2000) 8557–8560.
[7] Z.M. Zhu, N.Z. Liu, G.H. Li, H.X. Han, Z.P. Wang, S.Z. Wang, L. He, R.B. Ji, Y. Wu, J. Infrared Millimeter Waves 18 (1999) 13.
[8] S. Acharya, A.B. Panda, S. Efrima, Y. Golan, Adv. Mater. 19 (2007) 1105–1108.
[9] T. Matasuoka, Adv. Mater. 8 (1996) 469–472.
[10] B. Xiang, H.Z. Zhang, G.H. Li, F.H. Yang, F.H. Su, R.M. Wang, J. Xu, G.W. Lu, X.C. Sun, Q. Zhao, D.P. Yu, Appl. Phys. Lett. 82 (2003) 3330–3332.
[11] Z.D. Hu, X.F. Duan, M. Gao, Q. Chen, L.M. Peng, J. Phys. Chem. C 111 (2007) 2987–2991.
[12] U. Philipose, S. Yang, T. Xu, H.E. Ruda, Appl. Phys. Lett. 90 (2007) 063103.
[13] J.Q. Hu, Y. Bando, D. Golberg, Small 1 (2005) 95–99.
[14] S.L. Xiong, J.M. Shen, Q. Xie, Y.Q. Gao, Q. Tang, Y.T. Qian, Adv. Funct. Mater. 15 (2005) 1787–1792.
[15] X.T. Zhang, Z. Liu, Y.P. Leung, Q. Li, S.K. Hark, Appl. Phys. Lett. 83 (2003) 5533–5535.
[16] X.T. Zhang, Z. Liu, Q. Li, Y.P. Leung, K.M. Ip, S.K. Hark, Adv. Mater. 17 (2005) 1405–1410.
[17] X.T. Zhang, K.M. Ip, Z. Liu, Y.P. Leung, Q. Li, S.K. Hark, Appl. Phys. Lett. 84 (2004) 2641–2643.
[18] Y. Jiang, X.M. Meng, W.C. Yiu, J. Liu, X. Ding, C.S. Lee, S.T. Lee, J. Phys. Chem. B 108 (2004) 2784–2787.
[19] Y. Cai, S.K. Chan, I.K. Sou, Y.F. Chan, D.S. Su, N. Wang, Adv. Mater. 18 (2006) 109–114.
[20] Y. Cai, S.K. Chan, I.K. Sou, Y.F. Chan, D.S. Su, N. Wang, Small 3 (2007) 111–115.
[21] R. Solanki, J. Huo, J.L. Freeouf, Appl. Phys. Lett. 81 (2002) 3864–3866.
[22] A.S. Segal, A.N. Vorobev, S.Yu. Karpov, E.N. Mokhov, M.G. Ramm, M.S. Ramm, A.D. Roenkov, Yu.A. Vodakov, Yu.N. Makarov, J. Cryst. Growth 208 (2000) 431–441.
[23] S.Yu. Karpov, Yu.N. Makarov, M.S. Ramm, R.A. Talalaev, Mater. Sci. Eng. B 46 (1997) 340–344.
[24] C. Wetzel, D. Volm, B.K. Meyer, K. Pressel, S. Nilsson, E.N. Mokhov, P.G. Baranov, Appl. Phys. Lett. 65 (1994) 1033–1035.
[25] P.G. Baranov, E.N. Mokhov, A.O. Ostroumov, M.G. Ramm, M.S. Ramm, V.V. Ratnikov, A.D. Roenkov, Y.A. Vodakov, A.A. Wolfson, G.V. Saparin, D.V. Zimina, Y.N. Makarov, H. Juergensen, MRS Internet J.Nitride Semicond. Res. 50 (1998) 1.
[26] S.Yu. Karpov, Yu.N. Makarov, E.N. Mokhov, M.G. Ramm, M.S. Ramm, A.D. Roenkov, R.A. Talalaev, Yu.A. Vodakov, J. Cryst. Growth 173 (1997) 408–416.
[27] J.K. Jian, C. Wang, M. Lei, Z.H. Zhang, T.M. Wang, X.L. Chen, Appl. Surf. Sci. 254 (2008) 6637–6641.
[28] M. Lei, B. Song, X. Guo, W.H. Tang, Appl. Surf. Sci. 255 (2008) 2040–2045.
[29] D.B. Laks, C.G. Van de Walle, G.F. Neumark, P.E. Blochl, S.T. Pantelides, Phys. Rev. B 45 (1992) 10965–10978.
[30] U. Philipose, T. Xu, P. Sun, H.E. Harry, Y.Q. Ruda, K.L. Wang, Kavanagh, J. Appl. Phys. 100 (2006) 084316.
[31] U. Philipose, P. Sun, T. Xu, H.E. Harry, L. Ruda, K.L. Yang, Kavanagh, J. Appl. Phys. 101 (2007) 014326.
[32] K. Shahzad, J. Petruzzello, D.J. Olego, D.A. Cammack, Appl. Phys. Lett. 57 (1992) 2452–2454.
[33] B. Buda, C. Wang, W. Wrede, O. Leifeld, D.J. As, D. Schilora, L. Lischka, Semicond. Sci. Technol. 13 (1998) 921–926.